microRNA-137 promotes apoptosis in ovarian cancer cells via the regulation of XIAP

Xiaodi Li[1,5], Wei Chen[2,5], Wenshu Zeng[1], Chunling Wan[3], Shiwei Duan[4] and Songshan Jiang*[,1]

[1]State Key Laboratory of Biocontrol, School of Life Sciences, Sun Yat-sen University, Guangzhou, China; [2]Department of Gynecology, The Second Affiliated Hospital of Guangzhou Medical University, Guangzhou, China; [3]Bio-X Institutes, Key Laboratory for the Genetics of Developmental and Neuropsychiatric Disorders (Ministry of Education), Shanghai Jiao Tong University, Shanghai, China and [4]Medical Genetics Center, School of Medicine, Ningbo University, Ningbo, Zhejiang 315211, China

Background: microRNAs (miRNAs) have regulatory roles in various cellular processes, including apoptosis. Recently, X-linked inhibitor of apoptosis protein (XIAP) has been reported to be dysregulated in epithelial ovarian cancer (EOC). However, the mechanism underlying this dysregulation is largely unknown.

Methods: Using bioinformatics and a literature analysis, a panel of miRNAs dysregulated in EOC was chosen for further experimental confirmation from hundreds of miRNAs that were predicted to interact with the XIAP 3′UTR. A dual-luciferase reporter assay was employed to detect the interaction by cellular co-transfection of an miRNA expression vector and a reporter vector with the XIAP 3′UTR fused to a *Renilla* luciferase reporter. DAPI and TUNEL approaches were used to further determine the effects of an miR-137 mimic and inhibitor on cisplatin-induced apoptosis in ovarian cancer cells.

Results: We identified eight miRNAs by screening a panel of dysregulated miRNAs that may target the XIAP 3′UTR. The strongest inhibitory miRNA, miR-137, suppressed the activity of a luciferase reporter gene fused with the XIAP 3′UTR and decreased the levels of XIAP protein in SKOV3 ovarian cancer cells. Furthermore, forced expression of miR-137 increased cisplatin-induced apoptosis, and the depressed expression of miR-137 decreased cisplatin-induced apoptosis in SKOV3 and primary EOC cells. Consistently, the disruption of miR-137 via CRISPR/Cas9 inhibited apoptosis and upregulated XIAP in A2780 cells. Furthermore, the effect of miR-137 on apoptosis could be rescued by XIAP in SKOV3 cells. In addition, miR-137 expression is inversely correlated with the level of XIAP protein in both ovarian cancer tissues and cell lines.

Conclusions: Our data suggest that multiple miRNAs can regulate XIAP via its 3′UTR. miR-137 can sensitise ovarian cancer cells to cisplatin-induced apoptosis, providing new insight into overcoming drug resistance in ovarian cancer.

Despite a variety of advances in surgical techniques and chemotherapy approaches, ovarian cancer remains the most lethal gynaecologic malignancy, mainly because of late diagnosis and the development of resistance to standard chemotherapy such as platinum-based drugs (Holcik *et al*, 2000; Chan *et al*, 2009; van Jaarsveld *et al*, 2013; Borley and Brown, 2015). Apart from being an efficient drug for treating ovarian cancer, cisplatin is also one of the most commonly used ones; it causes cytotoxicity by interfering with the apoptotic pathways (Kurzeder *et al*, 2006). In this context, it is crucial to explore novel therapeutic approaches and targets to prevent or reduce drug resistance, thus enhancing the therapeutic efficiency of ovarian cancer.

miRNAs are a large class of tiny non-coding RNAs that are endogenously encoded and negatively regulate gene expression via binding to the 3′UTR regions of target mRNAs, leading to mRNA translational repression or degradation (Bartel, 2004; Lund *et al*, 2004).

It is reported that more than 60% of human protein-coding genes have been regulated by miRNAs (Friedman *et al*, 2009). These miRNAs function extensively in many cellular processes such as proliferation, metastasis and apoptosis (He and Hannon, 2004; Miska, 2005; Cui *et al*, 2016). For example, miR-340 can inhibit proliferation and induce apoptosis by targeting multiple negative regulators of p27 in non-small cell lung cancer (Fernandez *et al*, 2015). Our previous studies showed that the miR-23a/24-2/27a cluster promotes cell invasion and metastasis through targeting Sprouty2 in breast cancer (Li *et al*, 2013), and miR-24, miR-27a and miR-155 promote cell proliferation by regulating MXI1 in glioma (Xu *et al*, 2013; Zhou *et al*, 2013a). Recently, several miRNAs have been reported to be associated with drug resistance (Zheng *et al*, 2010). Some miRNAs could alter the sensitivity of cancer cells to anti-cancer drugs through targeting genes related to apoptosis and drug resistance. Overexpressed miR-21 promotes drug resistance due to its regulation of PDCD4, TPM1, and MARCKS in prostate cancer cells (Li *et al*, 2009). The significantly upregulated miR-214 targets the 3′UTR of PTEN and activates the Akt pathway, leading to enhanced cell survival following cisplatin treatment in ovarian cancer (Yang *et al*, 2008). The impact on apoptosis and the resistance of these deregulated miRNAs offer new avenues for cancer treatment.

Inhibitors of apoptosis (IAPs) are a family of proteins that are involved in various biological functions, including the regulation of innate immunity and inflammation, cell proliferation, cell migration and cell apoptosis (Berthelet and Dubrez, 2013). X-linked inhibitor of apoptosis protein (XIAP), identified by Liston, is considered to be the most potent apoptotic regulator in mammalian cells (Lencz *et al*, 2013). It can inhibit caspase activity by directly binding to caspase-3, -7, and -9 in the apoptotic signalling pathway (Eckelman *et al*, 2006). XIAP blocks a considerable portion of the apoptosis pathway and is an attractive therapeutic target of cancers. In epithelial ovarian cancer, XIAP is reported to be upregulated, and the upregulation of XIAP may be partially responsible for the generation and development of ovarian cancer (Kleinberg *et al*, 2007; Wang *et al*, 2012). Therefore, it is urgent to investigate the molecular mechanism of XIAP dysregulation in ovarian cancer.

Clustered regularly interspaced short palindromic repeats (CRISPR) and CRISPR-associated endonuclease 9 (Cas9), a novel genome editing system derived from Streptococcus pyogenes, can introduce double-strand breaks (DSBs) into cultured mammalian cells (Cho *et al*, 2013; Cong *et al*, 2013; Mali *et al*, 2013). Non-homologous end-joining (NHEJ) may participate in the repair of DSBs with a high frequency of insertions and deletions, leading to loss-of-function of the target gene. CRISPR/Cas9 has been applied to diverse functional genomics research because it is scalable, affordable, and easy to engineer (Deltcheva *et al*, 2011; Sapranauskas *et al*, 2011; Koike-Yusa *et al*, 2014). A component of the CRISPR/Cas9 system, single-guide RNA (sgRNA) with 20 nucleotides at the 5′ end complementary to the targeted region, can direct Cas9 endonucleases to produce DSBs. This new genome engineering tool provides an efficient and specific way to create new cell lines with loss-of-function of the gene that is essential for drug resistance in ovarian cancer.

In this study, we hypothesise that the abnormal expression of XIAP is caused, to some extent, by the deregulation of upstream miRNAs. By computational prediction and experimental confirmation, we demonstrated that eight miRNAs may regulate XIAP through screens of the interactions between the XIAP 3′UTR and 22 down-regulated miRNAs. Next, we chose miR-137 that has a strong effect in inhibiting XIAP for further confirmation. We investigated the roles of miR-137 in promoting apoptosis in ovarian cancer cells. We found that the overexpression of miR-137 can promote apoptosis induced by cisplatin, and the inhibition of miR-137 has a reverse effect. Knockout of the miR-137 gene via

CRISPR/Cas9 genome editing can decrease apoptosis induced by cisplatin in A2780 ovarian cancer cells. Furthermore, the increase in XIAP expression using lentivirus could rescue the phenotype of overexpression of miR-137. These results provide new insights into the role of miR-137, which may increase the sensitivity of ovarian cancer cells to cisplatin-induced apoptosis by regulating XIAP expression.

MATERIALS AND METHODS

Vector construction. To construct the luciferase reporter to screen the binding of miRNAs in the XIAP 3′UTR, 6.8 kb in length, we divided the whole XIAP 3′UTR into four fragments UTR1, UTR2, UTR3 and UTR4 (Figure 1). These four fragments, as well as the fragment containing two predicted miR-137 binding sites, and the predicted miR-137 binding site mutated fragments were fused to the *Renilla* luciferase reporter gene at the 3′UTR in the psiCHECK2 vector (Promega, Madison, WI, USA) with modified cloning sites. These constructs were named UTR1, UTR2, UTR3, UTR4, WT, site 1-MUT, site 2-MUT, and site $(1+2)$ MUT. All of the miRNA expression vectors containing the miRNA precursors used in this study were described previously (Zhou *et al*, 2013b). To overexpress XIAP, human XIAP cDNA without its native 3′UTR was cloned downstream of the CMV promoter in the lentiviral expression vector pCDH-CMV-MCS-EF1-copGFP (pCDH; System Biosciences, Mountain View, CA, USA), and the construct was named LV-XIAP. All of the primers employed above are listed in Supplementary Table S1. DNA sequencing was performed to confirm all of the constructs.

Analysis of the methylation of XIAP promoter. The methylation data of the XIAP promoter were from NCBI Gene Expression Omnibus (http://www.ncbi.nlm.nih.gov/geo/query/acc.cgi?acc= GSE51688). The β value ($\beta =$ signal B/(signal A + signal B + 100)) was used to determine the methylation rate.

Cell lines, cell culture and patient samples. The HEK293T (293T) cell line was purchased from the American Type Culture Collection (ATCC, Manassas, VA, USA) and cultured with DMEM (Invitrogen, Carlsbad, CA, USA) supplemented with 10% fetal bovine serum (FBS) and penicillin/streptomycin (Invitrogen) (100 U ml^{-1}) in an incubator at 37 °C with 5% CO_2. Seven human ovarian cancer cell lines, A2780 and SKOV3 from ATCC and CAOV3, OVCAR3, ES-2, COC1 and COC1/DDP from the Cell Center of Chinese Academy of Medical Sciences (Beijing, China), were maintained in an incubator at 37 °C with 5% CO_2 in appropriate media supplemented with 10% FBS and antibiotics following the manual instructions. Primary epithelial ovarian cancer (EOC) cells were obtained from the malignant ascites of two patients as previously described (Sapi *et al*, 2004). All primary ovarian cancer tissues, which contained >70% cancer cells, were collected from patients during primary cytoreductive surgery. The pathological type of the patients' cancers was determined according to WHO criteria, and 35 ovarian cancer tissues including 21 serous adenocystic carcinoma and 14 mucinous adenocystic carcinoma were used in this study. Twenty-nine normal ovarian tissues were obtained from age-matched patients who underwent removal of the ovary due to cervical cancer or endometrial cancer. All patients signed a consent form and the use of all specimens was approved by the Ethics Committee of the Second Affiliated Hospital of Guangzhou Medical University (No. 2013034).

Transfection of siRNAs, miRNA mimics and inhibitors. All of the RNA oligonucleotides used in this study, including the miR-137 mimic and inhibitor, XIAP siRNAs (si-XIAP), and their cognate control RNAs, were purchased from GenePharma

(Shanghai, China). The RNA sequences mentioned above were as follows: miR-137 mimic: sense 5′-UUAUUGCUUAAGAAUACGC GUAG-3′ and antisense 5′-ACGCGUAUUCUUAAGCAAUAAUU-3′; mimic control: sense 5′-UUGUCCGAACGUGUCACGUU-3′ and antisense 5′-ACGUGACACGUUCGGAGAAUU-3′; miR-137 inhibitor: 5′-CUACGCGUAUUCUUAAGCAAUAA-3′; inhibitor control: 5′-CAGUACUUUUGUGUAGUACAA-3′; si-XIAP-1: sense 5′-CAUGCAGCUGUAGAUAGAUGGCAAU-3′, antisense 5′-AUU GCCAUCUAUCUACAGCUGCAUG-3′; si-XIAP-2: sense 5′-GUGG UAGUCCUGUUUCAGCUU-3′, antisense 5′-GCUGAAACAGG ACUACCACUU-3′; siRNA control: sense 5′-UUCUCCGAACGU GUCACGUU-3′, antisense 5′-ACGUGACACGUUCGGAG AAUU-3′. The control RNA contains random sequences and predicted no interactions in cells. A total of $100\,\text{nmol}\,l^{-1}$ of small RNAs, the miRNA mimic or inhibitor, was used to perform cell transfection with the X-tremeGENE siRNA Transfection Reagent (Roche, Basel, Swiss) according to the manufacturer's instructions. To estimate the transfection efficiency, Cy3 dye-labeled RNA oligonucleotides (Ribobio, Guangzhou, China) were transfected into both A2780 and SKOV3 cells. The transfection efficiency was estimated to be approximately 90% in both cell lines.

Dual-luciferase reporter assay. The dual-luciferase reporter assay was performed as previously described (Zhou et al, 2013b). Briefly, 50 ng of luciferase reporter vector and 150 ng of either pLL3.7-miRNA or pLL3.7-miR-control vector were transfected into 1.5×10^4 293T cells in 96-well plates using FuGENE HD (Roche) according to the manufacturer's instructions. Forty-eight hours after transfection, the luciferase activity was measured using the dual-luciferase reporter assay system (Promega) following the manufacturer's instructions. Renilla luciferase activities were normalised to firefly luciferase activities.

Western blotting. The human ovarian cancer cells were lysed with RIPA lysis buffer (BioTeke, Beijing, China) 48 h after transfection. The protein concentration was determined using the bicinchoninic acid protein assay kit (Beyotime, Shanghai, China). Heat-denatured protein samples (20 μg per lane) were separated and then were transferred to a PVDF membrane (Millipore,
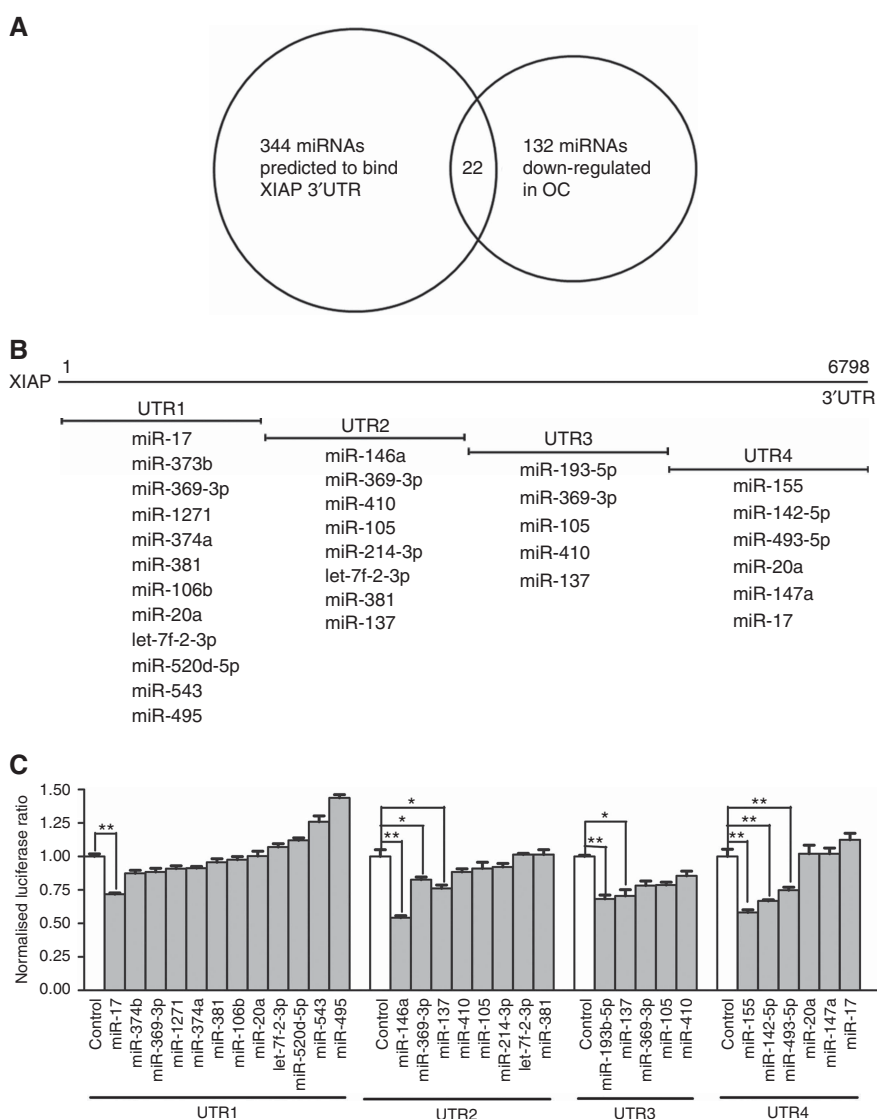
Figure 1. Screening for miRNAs targeting XIAP. (A) The Venn diagram shows the predicted XIAP 3′UTR binding miRNAs that were reported to be down-regulated in ovarian cancer. (B) Schematic diagram of the XIAP 3′UTR and miRNAs binding to the cognate fragments of XIAP 3′UTR. (C) Effects of 22 miRNAs on the activity of a luciferase reporter gene that is fused to four fragments of the XIAP 3′UTR in 293T cells using a dual-luciferase reporter assay. The luciferase activity of the transfected cells was measured 48 h post transfection. The results were presented as the relative luciferase activity and were normalised to the control, which was assigned a value of 1. The values represent the mean ± s.d. from three independent transfection experiments. Significant differences from the control value are indicated by *P<0.05 and **P<0.01.

Bedford, MD, USA) by 10% SDS-polyacrylamide gel electrophoresis. The membrane was incubated for 2 h at room temperature or incubated overnight at 4°C with a primary mouse polyclonal antibody against human XIAP (1 : 10 000; Santa Cruz Biotechnology, Santa Cruz, CA, USA) or mouse monoclonal antibody against human β-actin (1 : 3000; Abcam, Cambridge, MA, USA) and then was incubated for 1 h at room temperature with a goat anti-mouse secondary antibody (1 : 5000; Abcam, Cambridge, MA, USA). The bound antibody was assessed using enhanced chemiluminescence detection reagents (Pierce, Rockford, IL, USA), and the band intensities were quantified using Kodak Image Station 4000MM Pro (Kodak, Tokyo, Japan) according to the manufacturer's instructions.

RNA extraction and quantitative reverse transcription-PCR. Total RNA of the cell lines was extracted using Trizol (Invitrogen) and was reverse transcribed with ReverTra-Ace-α-Transcriptase (TOYOBO, Osaka, Japan). The expression of miR-137 and XIAP mRNA in the cell lines was quantified using the SYBR Premix Ex Taq II (Tli RNase H Plus) kit (Takara, Tokyo, Japan), and U6 snRNA and GAPDH were used as internal references, respectively. Quantitative PCR was performed using the LightCycler 480 Real-Time PCR system (Roche). The data were analysed using LightCycler 480 Software Version 1.5.

MTT assay. SKOV3 cells (1×10^4) were seeded in a 96-well plate and were transfected with miR-137 mimic or mimic control after 24 h. A series of concentration of cisplatin were added into culture medium for 48 h, and then 10 μl of 5 mg ml^{-1} of MTT reagent (Sigma, St Louis, MO, USA) per well was added to the medium, and the plate was incubated for 4 h in an incubator at 37 °C with

5% CO_2. One-hundred microliters of DMSO per well were added, and, then, the plate was thoroughly mixed for approximately 10 min. The spectrometric absorbance of the samples at 490 nm was measured on a microplate reader (BioTek, Winooski, VT, USA). The IC_{50} value was calculated graphically as a comparison to the growth of the control group.

4′,6-Diamidino-2-phenylindole staining of cells. SKOV3 cells or primary EOC cells were seeded (1.5×10^4 cells per well for each) in a 48-well plate and were transfected with the miR-137 mimic or mimic control. Sixteen to twenty-four hours after transfection, cisplatin (10 μM) was added to the medium. Twenty-four or forty-eight hours after the addition of cisplatin, SKOV3 or primary EOC cells were stained with 1 μg ml^{-1} 4′,6-diamidino-2-phenylindole (DAPI, Sigma). Apoptotic cells were observed under a fluorescence microscope, and the apoptotic ratio was calculated.

Terminal-deoxynucleotidyl transferase-mediated nick end labelling (TUNEL) assay. SKOV3 (1×10^4) cells were seeded in a 96-well plate, and transfection and cisplatin treatment was performed as described above. Forty-eight hours after cisplatin treatment, the cells were fixed with 4% methanol-free paraformaldehyde at 4 °C overnight, were exposed to 0.1% Triton X-100 (in 0.1% sodium citrate) for 2 min at 4 °C to permeabilize the cell membrane and then were rinsed twice with PBS. The terminal-deoxynucleotidyl transferase-mediated nick end labeling (TUNEL) reaction was performed according to the manufacturer's instructions (Roche). The apoptotic ratio was calculated as the ratio of the number of TUNEL-positive cells to the total number of DAPI-positive cells.

Virus generation and infection. Overall, 293T (8×10^5) cells were seeded in a 6-cm dish and then were co-transfected with
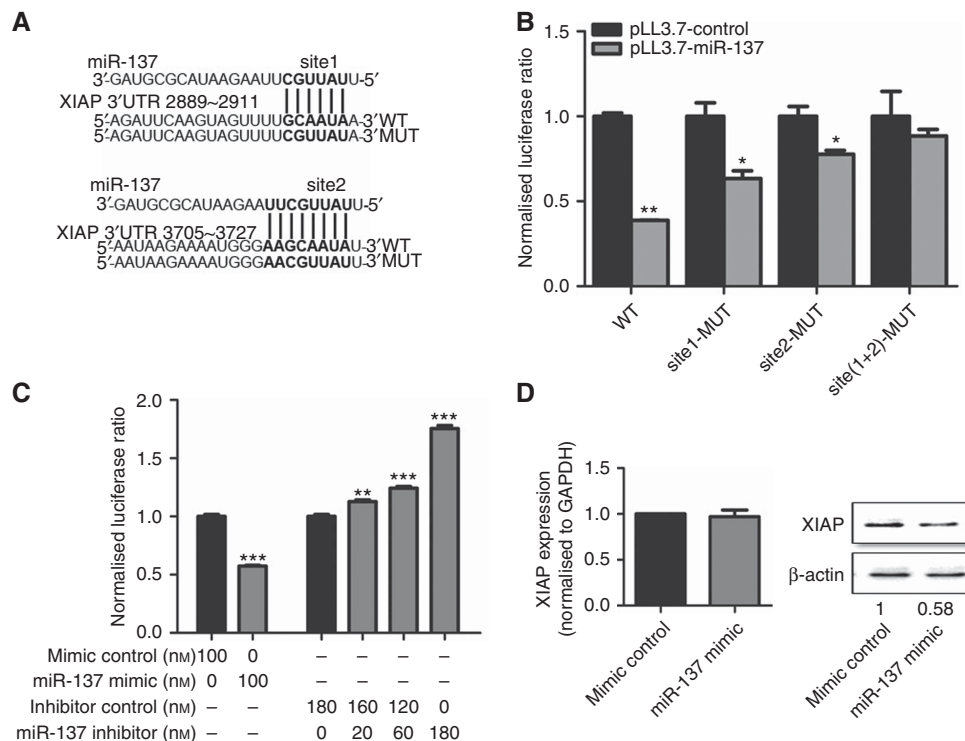
Figure 2. miR-137 reduces the XIAP protein level by directly targeting XIAP 3′UTR. (**A**) Two predicted target sites of miR-137 within the 3′UTR of XIAP and seed regions of the two sites, site 1 and 2, are mutated. (**B**) An empty vector or miR-137 expression vector (pLL3.7-miR-137) was co-transfected with the wild-type fragment of the XIAP 3′UTR containing the two sites in **A** (WT), the same fragment with one site mutated (site 1-MUT and site 2-MUT), or both sites mutated (site (1 + 2)-MUT), respectively. The luciferase activity of the transfected cells was measured 48 h post transfection. (**C**) The miR-137 mimic and inhibitor could down-regulate or up-regulate the relative luciferase ratio in SKOV3 cells, respectively. (**D**) After the transfection of the mimic control or miR-137 mimic into SKOV3 cells, the relative levels of XIAP mRNA and protein were measured by qRT-PCR and western blot, respectively. GAPDH and β-actin served as references for XIAP.

1.8 μg of packaging plasmid pPAX2, 0.6 μg of envelope plasmid pMD2.G and 2.5 μg of the XIAP expression vector LV-XIAP or empty vector pCDH with the transfection reagent Lipofectamine 2000 (Invitrogen) according to the manufacturer's instructions one day later. Viral supernatants were harvested and stored in a − 80 °C refrigerator 48 h after transfection. To improve the infection efficiency, 10 μg ml^{-1} polybrane was added before infection.

miR-137 genome editing via the CRISPR/Cas9 system. The sgRNAs targeting miR-137 were designed using CRISPRDESIGN (http://crispr.mit.edu/), and their corresponding DNAs were cloned into lentiCRISPR (pXPR_001) that contains the human codon-optimized SpCas9 coding sequence. The lentiCRISPR delivering Cas9 nuclease and miR-137-specific sgRNA were packed into lentivirus, and the A2780 ovarian cancer cells were infected with this lentivirus. Next, the tranduced cells were selected and enriched by applying 400 ng ml^{-1} puromycin to the medium. Single cells were sorted from the puromycin-selected population into 96-well plates and, after expansion, formed single-cell-derived cultures. PCR covering the sgRNA targeting region and Sanger sequencing were performed to examine miR-137 genome editing.

Statistical analysis. The data are presented as the mean ± standard deviation (± s.d.) of at least three separate experiments and were analysed using Student's t-test. P values < 0.05, 0.01, or 0.001 are indicated by *, **, or ***, respectively. Prism software (version 5.0; GraphPad Software, La Jolla, CA, USA) was used to analyse the data.

RESULTS

XIAP is targeted by multiple miRNAs. Several studies demonstrated that XIAP is highly expressed in ovarian cancer (Li et al, 2000; Wang et al, 2012). It is reported that the frequencies of SNPs in the XIAP promoter are not associated with cancer presentation (Kang et al, 2008; Ulybina et al, 2011; Xie et al, 2013). To explore the mechanism of the aberration expression of XIAP in ovarian cancer, both epigenetic modification, such as methylation, and posttranscriptional regulation were examined. We first checked whether the methylation frequency in the XIAP promoter is correlated with XIAP expression in ovarian cancer. As shown in Supplementary Figure S1, there is no significant difference in promoter methylation between ovarian cancer cell lines and normal ovarian cell lines using the database from NCBI Gene Expression Omnibus. Next, we hypothesised that some miRNAs, especially down-regulated miRNAs, might be responsible for the high expression of XIAP in ovarian cancer. To investigate which miRNAs might target XIAP, we predicted potential XIAP-binding miRNAs using TargetScan 5.1, DIANA LAB, microRNA and miRDB algorithms (Lewis et al, 2003; John et al, 2004) and found that 344 miRNAs were predicted to target the XIAP 3′UTR (Figure 1A). To identify the miRNAs that may down-regulate XIAP under pathogenic conditions, we searched for miRNAs that are down-expressed in ovarian cancer according to recent publications (Iorio et al, 2007; Dahiya et al, 2008; Yang et al, 2008; Li et al, 2010; Nagaraja et al, 2010; Guo et al, 2013), and 132 miRNAs were reported to be down-regulated in ovarian cancer. Among the 132 miRNAs, 22 were both predicted to target XIAP and were down-regulated in ovarian cancer (Figure 1A). We next tested all of these 22 miRNAs using a dual-luciferase assay through co-transfection into 293T cells of an miRNA expression vector containing miRNA precursor (pre-miRNA) available in our miRNA expression library (Zhou et al, 2013b) and a psiCHECK2 vector containing a Renilla luciferase reporter gene fused with their cognate fragment of the XIAP 3′UTR (UTR1-4). Eight miRNAs were determined to repress the activity of luciferase (Student's t-

test, P < 0.05) (Figure 1B and C), and the inhibiting effects of miR-137 (combination of two experiments with UTR2 and UTR3), miR-155, miR-142 and miR-146a are obvious. Because miR-137 has the most potent activity and is reported to be down-regulated in several cancers, including ovarian cancer (Bier et al, 2013; Chen et al, 2013; Guo et al, 2013; Takwi et al, 2014), we chose miR-137 for further experiments.

XIAP is a direct downstream target of miR-137. To determine whether miR-137 recognises the two predicted sites (2889–2911, 3705–3727), we constructed the XIAP 3′UTR reporter with the two sites in one fragment. Next, the wild-type fragment, the seed region-mutated fragments for site 1, site 2, and double-mutated fragment for both sites, were cloned downstream of the Renilla luciferase reporter gene in the psiCHECK2 vector, respectively (Figure 2A and B). Each of the constructs was co-transfected into 293T cells with the miR-137 expression vector pLL3.7-miR-137, and the empty vector (pLL3.7-miR control) was used as a control. By testing the luciferase activity, we found that the ability of miR-137 to inhibit XIAP was attenuated through a mutation of either of the two sites or was abrogated through mutations of both sites. The inhibiting effect of site 2 was stronger than that of site 1 (Figure 2B). Subsequently, we employed the miRNA mimic and inhibitor to further determine the regulation of miR-137 in the inhibition of XIAP. The luciferase activity of 293T cells co-transfected with the luciferase reporter construct fused with the wild-type fragment and miR-137 mimic decreased significantly compared with that co-transfected with the mimic control. Consistently, the luciferase activity of the 293T cells co-transfected with the miR-137 inhibitor and reporter construct was increased compared with that co-transfected with the inhibitor control in a dose-dependent manner (Figure 2C).
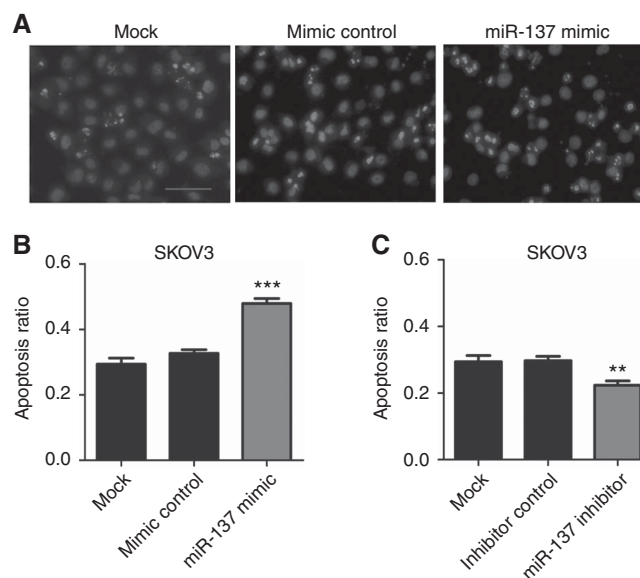
Figure 3. DAPI staining identifies that miR-137 promotes cell apoptosis in SKOV3 cells. (A, B) SKOV3 cells were transfected with a mock, a mimic control, or a miR-137 mimic construct as indicated, and the cells were then treated with 10 μM cisplatin 24 h later. DAPI staining of the cells' apoptotic nuclei was performed after 48 h. Representative experiments are shown in A (scale bar, 100 μm), and the statistical results are shown in B. The apoptotic rate was expressed as the ratio of the number of cells with apoptotic nuclei to the total number of DAPI-positive cells, as shown in B. (C) SKOV3 cells were transfected with the inhibitor control or miR-137 inhibitor, and the apoptotic rate was shown. The average values ± s.d. of three separate experiments were plotted, and significant differences from the control value are indicated by **P < 0.01 and ***P < 0.001.

To determine whether miR-137 can regulate endogenous XIAP expression, A2780 ovarian cancer cells were transfected with the miR-137 mimics and control, respectively. Quantitative reverse transcription-PCR (qRT-PCR) confirmed that miR-137 was overexpressed. Western blot analysis showed that miR-137 down-regulated the protein level of endogenous XIAP; however, the level of XIAP mRNA was not changed (Figure 2D). Altogether, these data suggest that miR-137 directly targets XIAP via the predicted cognate sites at the 3′UTR in 293T and SKOV3 ovarian cancer cells.
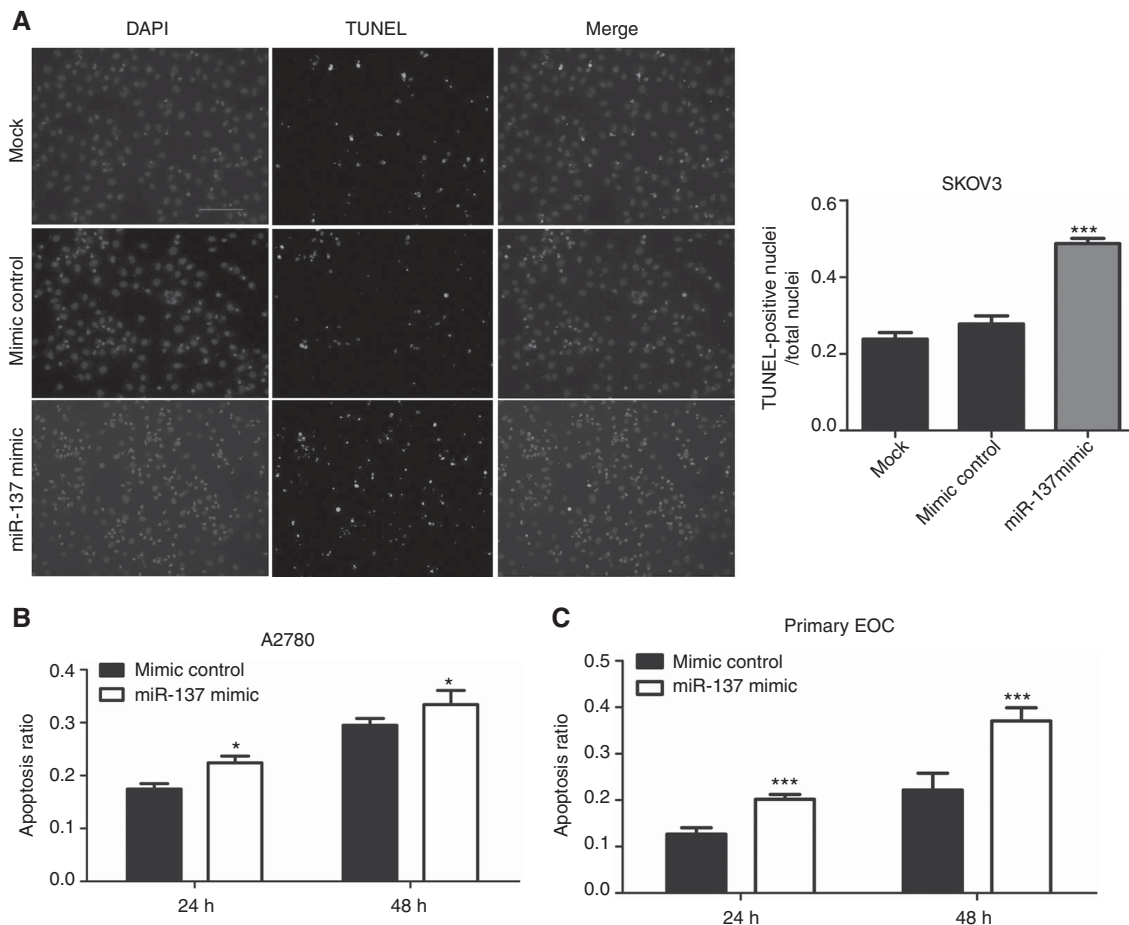
miR-137 increases the sensitivity of ovarian cancer cells to cisplatin-induced apoptosis. To investigate the apoptotic effects of miR-137 in ovarian cancer, SKOV3 cells were transfected with a mimic control and mimic of miR-137, respectively, and then were treated with $10 \mu M$ cisplatin 24 h later. We observed apoptotic nuclei of the cells with DAPI staining using fluorescence microscopy 48 h after the addition of cisplatin. Compared with the mock and mimic control, the apoptotic rates were significantly higher in the cells transfected with the miR-137 mimic (Figure 3A and B). Consistently, when the miR-137 inhibitor was transfected into SKOV3 cells, the apoptotic ratio was lower than that of the mock or control group (Figure 3C).

Furthermore, the effect of miR-137 in promoting cell apoptosis was confirmed in SKOV3 cells by the TUNEL assay. Compared

with the mimic control, the apoptotic rates were higher in the cells transfected with the miR-137 mimic (Figure 4A). The effect of miR-137 in promoting cell apoptosis was also supported by the IC_{50} values of cisplatin in SKOV3 cells transfected with the miR-137 mimic. As shown in Supplementary Figure S2, the MTT cell viability assay indicated that the IC_{50} values of cisplatin decreased significantly due to transfection with the miR-137 mimic, suggesting that miR-137 is effective in increasing the sensitivity of SKOV3 ovarian cancer cells to cisplatin-induced apoptosis.

In addition, DAPI staining experiments were performed with A2780 ovarian cancer cells and primary cultured epithelial ovarian cancer (primary EOC) cells isolated from patient ascites. Apoptosis was observed in A2780 and primary EOC cells treated with $10 \mu M$ cisplatin at 24 and 48 h (Figure 4B and C). The apoptotic ratio was notably higher in the cells transfected with the miR-137 mimic at 24 and 48 h. Altogether, these data suggest that miR-137 can increase the sensitivity of ovarian cancer cells to cisplatin-induced apoptosis.

Disruption of miR-137 via CRISPR/Cas9 up-regulates XIAP and decreases apoptosis in A2780 cells. To further confirm the effect of miR-137 in ovarian cancer cells, the CRISPR/Cas9 system was used to perform miR-137 genome editing. We design three small

Figure 4. miR-137 increases the sensitivity of ovarian cancer cells to cisplatin-induced apoptosis. (A) SKOV3 cells were transfected with a mock, a mimic control, or a miR-137 mimic, and then the cells were treated with $10 \mu M$ cisplatin 24 h later. DAPI staining and TUNEL labelling of the cells' apoptotic nuclei were performed after 48 h. The apoptotic rate was expressed as the ratio of the number of the cells with TUNEL-positive nuclei to the total number of DAPI-positive cells. Representative experiments (scale bar, $100 \mu m$) and the statistical results are shown in **A**. (**B**, **C**) A2780 (**B**) and primary EOC (**C**) cells were transfected with a mimic control and a miR-137 mimic as indicated, and the cells were treated with $10 \mu M$ cisplatin 24 h later. DAPI staining of the cells' apoptotic nuclei was performed after 24 and 48 h. The apoptotic rate was expressed as the ratio of the number of the cells with apoptotic nuclei to the total number of DAPI-positive cells. The average values ± s.d. of three separate experiments were plotted, and significant differences from the control value are indicated by *$P<0.05$, ***$P<0.001$.

guide RNAs (sgRNAs) that target different locations of the miR-137 genome, including the upstream, downstream and exact region of mature miR-137 (Figure 5A). To obtain the strongest effect with the disruption of the miR-137 genomic sequence, we measured the expression level of miR-137 in seven ovarian cell lines using qRT-PCR and chose A2780, with the highest level of miR-137 expression, to perform miR-137 genome editing (Figure 5B). Following the schedule (Figure 5C), A2780 cells were infected with the lentiviral particle of CRISPR/Cas9 (lentiCRISPR) that over-expresses, respectively, sgRNA and Cas9 endonuclease, and then were selected with puromycin. The clones of single cells with miR-137 disruption were identified through PCR and sequencing of the miR-137 genomic fragment. The sequences of the three clones with both miR-137 alleles disrupted, #1, #2 and #3, are shown in Figure 5D, and the Sanger sequencing results for #1 is shown in Supplementary Figure S3. These clones cannot express miR-137 as determined by qRT-PCR. These above findings indicated that we could successfully disrupt miR-137 genomic DNA in A2780 ovarian cancer cells. Next, we used these clones to test whether miR-137 regulated XIAP and the effects of miR-137 on apoptosis. The results of western blot assay showed that the protein levels of XIAP were down-regulated in all three clones (Figure 5E). To investigate the effects of miR-137 on apoptosis, two clones, #1 and #2, were treated with $10\,\mu M$ cisplatin for 48 h. We observed that, compared with the wild-type A2780 control cells, the apoptotic rates were significantly lower in the cells of both #1 and #2
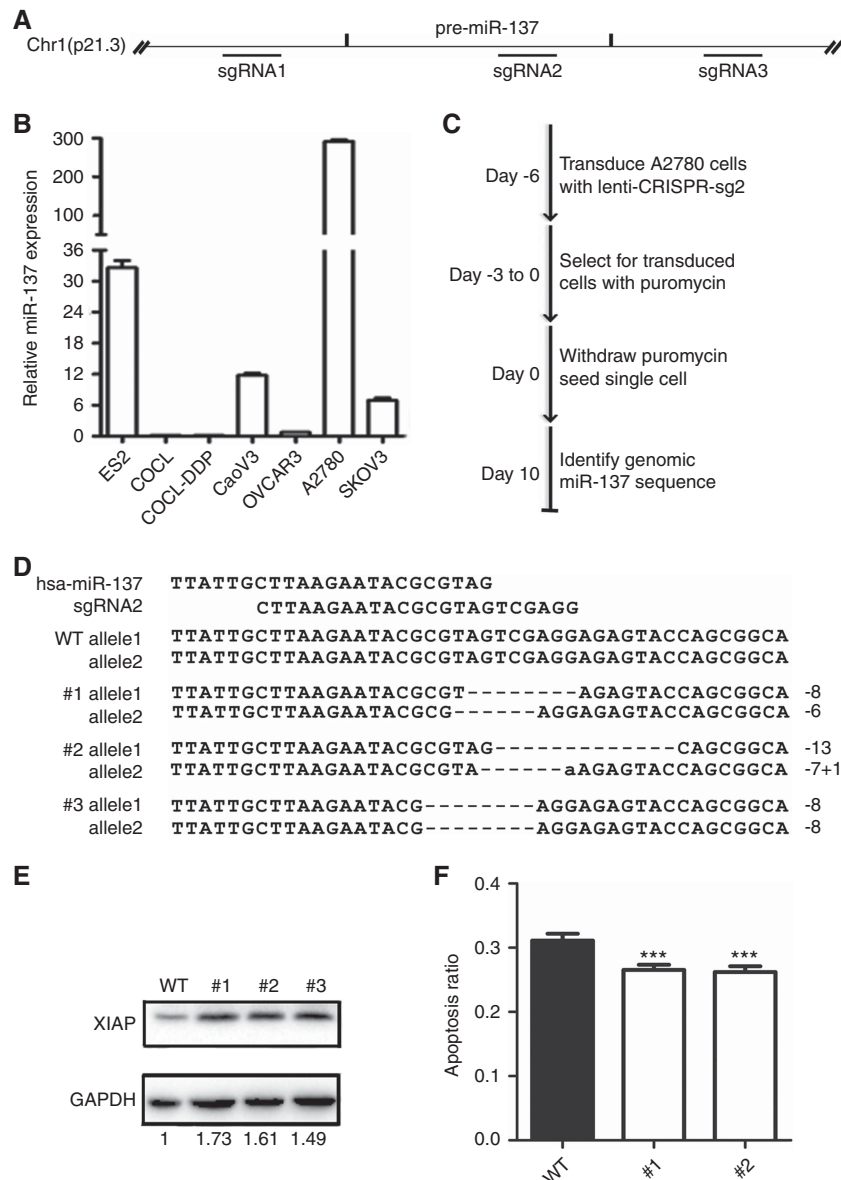

Figure 5. miR-137 knockout via CRISPR/Cas9 genome editing up-regulates XIAP protein and inhibits apoptosis in A2780 cells. (A) The location of three designed sgRNAs that target genomic miR-137. (B) miR-137 expression in several ovarian cancer cell lines. (C) Timeline of miR-137 genome editing in the A2780 cell line. (D) Representative sequences of the mutated alleles from #1, #2, #3 single-cell clones derived from sgRNA2. Black dashes, deleted bases; lowercase bases, insertions. (E) XIAP protein levels of the four clones and wild-type A2780 cells (WT) in D. (F) The apoptosis ratios of the wild-type A2780 cells (A2780 WT) and #1 and #2 clones were determined as shown in Figure 4A. The same amount of wild-type A2780 cells (WT) and cells of the #1 and #2 clones were seeded in 48-well plates, followed by treatment with $10\,\mu M$ cisplatin 24 h later. DAPI staining of the cells' apoptotic nuclei was performed after 48 h. The apoptotic rate was expressed as the ratio of the number of the cells with apoptotic nuclei to the total number of DAPI-positive cells. The average values ± s.d. of three separate experiments were plotted, and significant differences from the control value are indicated by ***$P < 0.001$.

(Figure 5F), indicating that the clones with miR-137 disrupted seem less sensitive than A2780 cells to the same concentration of cisplatin. These data revealed that the disruption of the miR-137 genomic sequence affected the expression of miR-137 and increased the protein level of XIAP, leading to the decrease in the sensitivity to cisplatin-induced apoptosis in A2780 cells.

XIAP attenuates the effect of miR-137 on apoptosis. To test whether XIAP can protect ovarian cancer cells from cisplatin-induced apoptosis, we forced XIAP expression in SKOV3 cells through lentiviral infection and decreased XIAP expression in SKOV3 and primary EOC cells through siRNA transfection, The results of DAPI staining suggest that XIAP can protect SKOV3 and primary EOC cells from cisplatin-induced apoptosis (Supplementary Figure S4). To further validate the hypothesis that the effect ofmiR-137 in sensitising ovarian cancer cells to cisplatin-induced apoptosis is mediated by XIAP, rescue experiments were carried out for miR-137. SKOV3 cells were first infected with different amounts of lentivirus expressing XIAP (multiplicities of infection (MOI): 1 or 2), and then the cells were transfected with 100 nM of the miR-137 mimic 24 h later. The DAPI staining data indicated that no difference between the MOI 1 experimental and control groups (Figure 6A and B), implying that XIAP inhibited the effect of miR-137 in enhancing apoptosis in SKOV3 cells. With a MOI of 2, the enhancing effect of miR-137 was strongly inhibited. Consistently, the SKOV3 cells co-transfected with 50 nM of the miR-137 inhibitor and 50 nM of XIAP siRNA (si-XIAP-2) showed no difference between the experimental and control groups (Figure 6C). Furthermore, when the amount of co-transfected XIAP siRNA was decreased, the inhibiting effect of the miR-137 inhibitor was only partially rescued. Altogether, these results further suggest that XIAP is one of the functional downstream targets of miR-137 in promoting ovarian cancer cell apoptosis.

miR-137 is inversely correlated with the level of XIAP protein in ovarian cancer. Given that miR-137 functionally regulates XIAP expression at the protein level but not at the mRNA level in ovarian cancer cells, we further determined whether the expression level of miR-137 is correlated with the protein level of XIAP in both ovarian cancer tissues and cell lines. Thirty-five EOC tissues of grade I-III, as well as 29 age-matched normal ovarian tissues were used for the analysis. The expression levels of miR-137 and XIAP proteins were determined by qRT-PCR and western blot, respectively. Compared with normal ovarian tissues, the expression
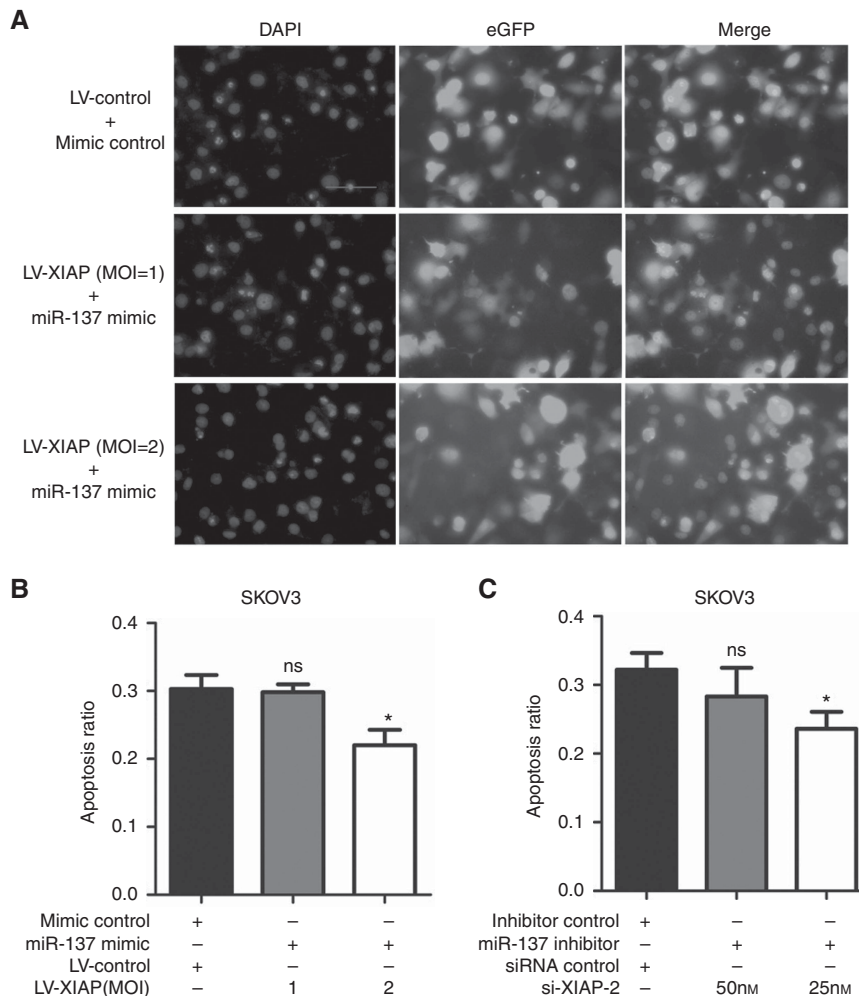
Figure 6. XIAP rescues the effect of miR-137 on apoptosis in SKOV3 cells. (**A**, **B**) SKOV3 cells were infected with lentivirus expressing XIAP (LV-XIAP) with MOI of 1 or 2 or with a control (LV-control), with further transfection of the miR-137 mimic or mimic control. The cells were then treated with $10 \mu g \, ml^{-1}$ cisplatin to trigger apoptosis. DAPI staining was performed as previously described in Figure 3. Representative experiments are shown in **A** (scale bar, $100 \mu m$) and the statistical results are shown in **B**. (**C**) SKOV3 cells were co-transfected with miR-137 mimic or mimic control, and si-XIAP-2 or siRNA control. The apoptotic ratios are shown in a histogram. The average values ± s.d. of three separate experiments were plotted, and significant differences from the control value are indicated by *$P < 0.05$.
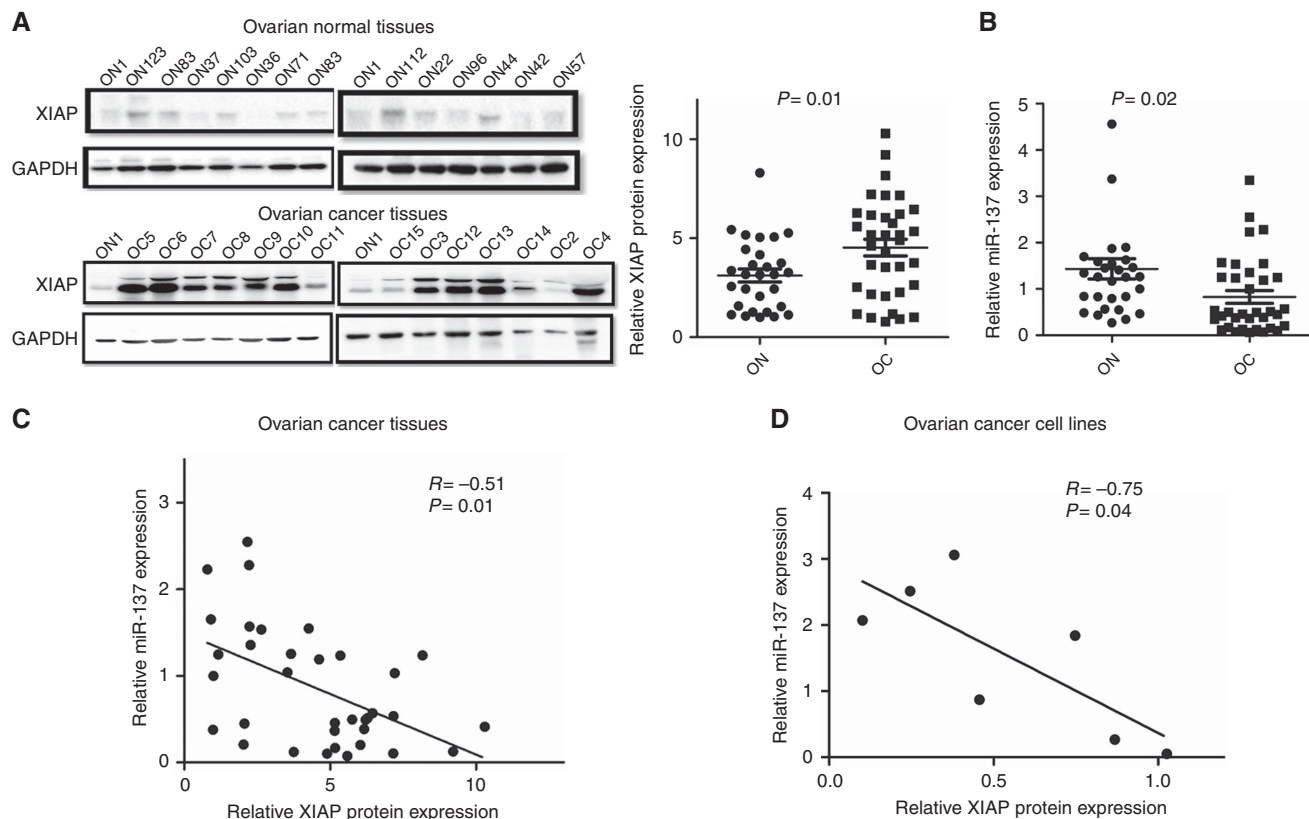
Figure 7. Correlations between the levels of miR-137 and XIAP protein in ovarian cancer. (A) XIAP protein levels in 35 ovarian cancer tissues (OC) and 29 normal ovarian tissues (ON) were determined by western blot. Representative experiments are shown in the left panel and the statistical results are shown in the right panel. GAPDH served as an internal loading reference and the sample ON1 in the first lane of each gel was used as control for normalisation. (B) miR-137 expression in 35 ovarian cancer tissues and 29 normal ovarian tissues, with U6 serving as internal reference. (C, D) Correlation between the levels of XIAP protein and miR-137 in ovarian cancer tissues (C) and ovarian cancer cell lines (D) was evaluated using Pearson rank correlation analysis.

of XIAP is upregulated, whereas miR-137 is down-regulated, in ovarian cancer tissues (Figure 7A and B). Using Pearson's correlation analysis, we obtained a statistically inverse correlation between the levels of miR-137 and XIAP proteins ($R = -0.51$, $P = 0.01$) in all 35 cancer tissues (Figure 7C). In addition, the levels of miR-137 and XIAP proteins in the seven ovarian cancer cell lines (CAOV3, OVCAR3, SKOV3, A2780, ES-2, COC1, and COC1/DDP) were measured and a similar inverse correlation was obtained by Pearson's correlation analysis (Figure 7D). Altogether, these results suggest that miR-137 expression is inversely correlated with the level of XIAP protein in both ovarian cancer tissues and cell lines.

DISCUSSION

Deregulation of XIAP often occurs in cancers (Li et al, 2000; Sasaki et al, 2000; Tamm et al, 2000). In pancreatic cancer, XIAP is overexpressed and correlates to resistance to cancer drugs, and the down-regulation of XIAP by siRNA interference confirmed that XIAP affects the response to the anti-cancer drugs (Lopes et al, 2007). It was reported that the level of XIAP expression was increased in ovarian cancer (Potkin et al, 2009; McGrath et al, 2013; Shibata et al, 2013). The reduction of XIAP expression through RNAi sensitises cancer cells to several diverse chemotherapeutics (McManus et al, 2004), providing a new insight into the effect of XIAP on drug resistance and the significance to uncover the mechanism of the dysregulation of XIAP in ovarian cancer.

Very few gene point mutations of XIAP have been reported in cancers. Although there are some variations, most of them do not account for the distinct expression of XIAP in tumours and cancer cells (Kang et al, 2008; Ulybina et al, 2011; Xie et al, 2013). In addition, certain reports have suggested that XIAP is regulated by miRNA at the posttranscriptional level via binding to the 3'UTR of XIAP mRNA in some cancers (Zhu et al, 2012; Xie et al, 2013). To investigate the mechanism of XIAP dysregulation in ovarian cancer, we focused on abnormal miRNAs especially those down-regulated in ovarian cancer. We select 22 miRNAs that were reported to be down-regulated in ovarian cancer in the literature and that were predicted to target the 3'UTR of XIAP mRNA through several algorithms. Among the eight miRNAs with inhibiting effects found in luciferase reporter screens, we selected miR-137, which significantly regulates the 3'UTR of XIAP mRNA, for further experiments. For the first time, we report that miR-137 can regulate XIAP in 293T and ovarian cancer cells. Several lines of evidence support a direct interaction between miR-137 and the XIAP 3'UTR. First, the human XIAP 3'UTR contains two putative miR-137 binding sites with prominent seed matches (Figures 1B and 2A). Second, miR-137 can suppress the activity of the luciferase reporter gene fused to the 3'UTR of XIAP mRNA. While the target sites were mutated, no significant changes have been shown in luciferase activities. Third, synthetic miR-137 mimic could repress the endogenous expression of XIAP at the protein level in SKOV3 ovarian cancer cells. Fourth, the expression of XIAP cDNA without its native 3'UTR can rescue the apoptosis-promoting effect of miR-137, and the decrease in XIAP with siRNA can also rescue the inhibiting effect of miR-137. Fifth, miR-

137 expression is inversely correlated with the level of XIAP protein in both ovarian cancer tissues and cell lines. In addition, cloning cells with miR-137 disruption via CRISPR/Cas9 genome editing show that the level of XIAP protein is increased, suggesting XIAP is regulated by miR-137 in ovarian cancer.

miRNAs are important and ubiquitous in eukaryotes, and combinatorial regulation by miRNAs makes it possible that a given mRNA is regulated by multiple miRNAs and a given miRNA could target multiple mRNAs (Krek *et al*, 2005; Rajewsky, 2006). p21Cip1/Waf1, a member of the Cip/Kip family of cyclin kinase inhibitors, is inhibited by 28 miRNAs at the translational level (Wu *et al*, 2010). Both miR-137 and miR-2008 promote ROS production and the clearance of pathogenic microorganisms by regulating the common target AjBHMT (Zhang *et al*, 2015). Our previous study showed that miR-24-3p and miR-27a-3p can enhance cell proliferation in glioma cells via cooperative regulation of MXI1 (Xu *et al*, 2013). Our current study provides the first identification and demonstration that multiple miRNAs through their down-regulation function can regulate XIAP, thus enhancing our understanding of the function and regulation of XIAP in ovarian cancer cells. Such combinational regulation of miRNAs facilitates the maintenance of the stable expression of the target gene under physiological conditions. However, under pathological conditions, multiple miRNAs might be dysregulated such as several of the miRNAs in our study, and their down-regulation might be one of the reasons for diseases such as cancers.

In summary, we found that several miRNAs, including miR-137, can target the XIAP gene through a systematic screen, and miR-137 decreased XIAP expression through special sites in the XIAP 3′UTR. Our results that miR-137 promoted epithelial ovarian cancer cells to undergo cisplatin-induced apoptosis suggest that miR-137 is involved in the regulation of apoptosis in ovarian cancer cells and that miR-137 is a promising potential therapeutic target. Therefore, exploiting therapy based on miR-137 may be beneficial for the clinical treatment of ovarian cancer and overcoming drug resistance.

ACKNOWLEDGEMENTS

CONFLICT OF INTEREST

The authors declare that no conflict of interest exist.

REFERENCES

Bartel DP (2004) MicroRNAs: genomics, biogenesis, mechanism, and function. *Cell* **116**(2): 281–297.

Berthelet J, Dubrez L (2013) Regulation of apoptosis by inhibitors of apoptosis (IAPs). *Cells* **2**(1): 163–187.

Bier A, Giladi N, Kronfeld N, Lee HK, Cazacu S, Finniss S, Xiang C, Poisson L, deCarvalho AC, Slavin S, Jacoby E, Yalon M, Toren A, Mikkelsen T, Brodie C (2013) MicroRNA-137 is downregulated in glioblastoma and inhibits the stemness of glioma stem cells by targeting RTVP-1. *Oncotarget* **4**(5): 665–676.

Borley J, Brown R (2015) Epigenetic mechanisms and therapeutic targets of chemotherapy resistance in epithelial ovarian cancer. *Ann Med* **47**: 1–11.

Chan DW, Liu VW, To RM, Chiu PM, Lee WY, Yao KM, Cheung AN, Ngan HY (2009) Overexpression of FOXG1 contributes to TGF-beta resistance through inhibition of p21WAF1/CIP1 expression in ovarian cancer. *Br J Cancer* **101**(8): 1433–1443.

Chen DL, Wang DS, Wu WJ, Zeng ZL, Luo HY, Qiu MZ, Ren C, Zhang DS, Wang ZQ, Wang FH, Li YH, Kang TB, Xu RH (2013) Overexpression of paxillin induced by miR-137 suppression promotes tumor progression and metastasis in colorectal cancer. *Carcinogenesis* **34**(4): 803–811.

Cho SW, Kim S, Kim JM, Kim JS (2013) Targeted genome engineering in human cells with the Cas9 RNA-guided endonuclease. *Nat Biotechnol* **31**(3): 230–232.

Cong L, Ran FA, Cox D, Lin S, Barretto R, Habib N, Hsu PD, Wu X, Jiang W, Marraffini LA, Zhang F (2013) Multiplex genome engineering using CRISPR/Cas systems. *Science* **339**(6121): 819–823.

Cui Y, Han J, Xiao Z, Chen T, Wang B, Chen B, Liu S, Han S, Fang Y, Wei J, Wang X, Ma X, Dai J (2016) The miR-20-Rest-Wnt signaling axis regulates neural progenitor cell differentiation. *Sci Rep* **6**: 23300.

Dahiya N, Sherman-Baust CA, Wang TL, Davidson B, Shih IeM, Zhang Y, Wood 3rd W, Becker KG, Morin PJ (2008) MicroRNA expression and identification of putative miRNA targets in ovarian cancer. *PloS one* **3**(6): e2436.

Deltcheva E, Chylinski K, Sharma CM, Gonzales K, Chao Y, Pirzada ZA, Eckert MR, Vogel J, Charpentier E (2011) CRISPR RNA maturation by trans-encoded small RNA and host factor RNase III. *Nature* **471**(7340): 602–607.

Eckelman BP, Salvesen GS, Scott FL (2006) Human inhibitor of apoptosis proteins: why XIAP is the black sheep of the family. *EMBO Rep* **7**(10): 988–994.

Fernandez S, Risolino M, Mandia N, Talotta F, Soini Y, Incoronato M, Condorelli G, Banfi S, Verde P (2015) miR-340 inhibits tumor cell proliferation and induces apoptosis by targeting multiple negative regulators of p27 in non-small cell lung cancer. *Oncogene* **34**(25): 3240–3250.

Friedman RC, Farh KK, Burge CB, Bartel DP (2009) Most mammalian mRNAs are conserved targets of microRNAs. *Genome Res* **19**(1): 92–105.

Guo J, Xia B, Meng F, Lou G (2013) miR-137 suppresses cell growth in ovarian cancer by targeting AEG-1. *Biochem Biophys Res Commun* **441**(2): 357–363.

He L, Hannon GJ (2004) MicroRNAs: small RNAs with a big role in gene regulation. *Nat Rev Genet* **5**(7): 522–531.

Holcik M, Yeh C, Korneluk RG, Chow T (2000) Translational upregulation of X-linked inhibitor of apoptosis (XIAP) increases resistance to radiation induced cell death. *Oncogene* **19**(36): 4174–4177.

Iorio MV, Visone R, Di Leva G, Donati V, Petrocca F, Casalini P, Taccioli C, Volinia S, Liu CG, Alder H, Calin GA, Menard S, Croce CM (2007) MicroRNA signatures in human ovarian cancer. *Cancer Res* **67**(18): 8699–8707.

John B, Enright AJ, Aravin A, Tuschl T, Sander C, Marks DS (2004) Human microRNA targets. *PLoS Biol* **2**(11): e363.

Kang HG, Lee SJ, Chae MH, Lee WK, Cha SI, Kim CH, Kam S, Park RW, Kim IS, Kim DS, Kim YC, Jung TH, Park JY (2008) Identification of polymorphisms in the XIAP gene and analysis of association with lung cancer risk in a Korean population. *Cancer Genet Cytogenet* **180**(1): 6–13.

Kleinberg L, Florenes VA, Silins I, Haug K, Trope CG, Nesland JM, Davidson B (2007) Nuclear expression of survivin is associated with improved survival in metastatic ovarian carcinoma. *Cancer* **109**(2): 228–238.

Koike-Yusa H, Li Y, Tan EP, Velasco-Herrera Mdel C, Yusa K (2014) Genome-wide recessive genetic screening in mammalian cells with a lentiviral CRISPR-guide RNA library. *Nat Biotechnol* **32**(3): 267–273.

Krek A, Grun D, Poy MN, Wolf R, Rosenberg L, Epstein EJ, MacMenamin P, da Piedade I, Gunsalus KC, Stoffel M, Rajewsky N (2005) Combinatorial microRNA target predictions. *Nat Genet* **37**(5): 495–500.

Kurzeder C, Sauer G, Deissler H (2006) Molecular targets of ovarian carcinomas with acquired resistance to platinum/taxane chemotherapy. *Curr Cancer Drug Targets* **6**(3): 207–227.

Lencz T, Guha S, Liu C, Rosenfeld J, Mukherjee S, DeRosse P, John M, Cheng L, Zhang C, Badner JA, Ikeda M, Iwata N, Cichon S, Rietschel M, Nothen MM, Cheng AT, Hodgkinson C, Yuan Q, Kane JM, Lee AT, Pisante A, Gregersen PK, Pe'er I, Malhotra AK, Goldman D, Darvasi A (2013) Genome-wide association study implicates NDST3 in schizophrenia and bipolar disorder. *Nat Commun* **4**: 2739.

Lewis BP, Shih IH, Jones-Rhoades MW, Bartel DP, Burge CB (2003) Prediction of mammalian microRNA targets. *Cell* **115**(7): 787–798.

Li J, Sasaki H, Sheng YL, Schneiderman D, Xiao CW, Kotsuji F, Tsang BK (2000) Apoptosis and chemoresistance in human ovarian cancer: is Xiap a determinant? *Biol Signals Recept* **9**(2): 122–130.

Li SD, Zhang JR, Wang YQ, Wan XP (2010) The role of microRNAs in ovarian cancer initiation and progression. *J Cell Mol Med* **14**(9): 2240–2249.

Li T, Li D, Sha J, Sun P, Huang Y (2009) MicroRNA-21 directly targets MARCKS and promotes apoptosis resistance and invasion in prostate cancer cells. *Biochem Biophys Res Commun* 383(3): 280–285.

Li X, Liu X, Xu W, Zhou P, Gao P, Jiang S, Lobie PE, Zhu T (2013) c-MYC-regulated miR-23a/24-2/27a cluster promotes mammary carcinoma cell invasion and hepatic metastasis by targeting Sprouty2. *J Biol Chem* 288(25): 18121–18133.

Lopes RB, Gangeswaran R, McNeish IA, Wang Y, Lemoine NR (2007) Expression of the IAP protein family is dysregulated in pancreatic cancer cells and is important for resistance to chemotherapy. *Int J Cancer* 120(11): 2344–2352.

Lund E, Guttinger S, Calado A, Dahlberg JE, Kutay U (2004) Nuclear export of microRNA precursors. *Science* 303(5654): 95–98.

Mali P, Yang L, Esvelt KM, Aach J, Guell M, DiCarlo JE, Norville JE, Church GM (2013) RNA-guided human genome engineering via Cas9. *Science* 339(6121): 823–826.

McGrath LM, Cornelis MC, Lee PH, Robinson EB, Duncan LE, Barnett JH, Huang J, Gerber G, Sklar P, Sullivan P, Perlis RH, Smoller JW (2013) Genetic predictors of risk and resilience in psychiatric disorders: a cross-disorder genome-wide association study of functional impairment in major depressive disorder, bipolar disorder, and schizophrenia. *Am J Med Genet B* 162B(8): 779–788.

McManus DC, Lefebvre CA, Cherton-Horvat G, St-Jean M, Kandimalla ER, Agrawal S, Morris SJ, Durkin JP, Lacasse EC (2004) Loss of XIAP protein expression by RNAi and antisense approaches sensitizes cancer cells to functionally diverse chemotherapeutics. *Oncogene* 23(49): 8105–8117.

Miska EA (2005) How microRNAs control cell division, differentiation and death. *Curr Opin Genet Dev* 15(5): 563–568.

Nagaraja AK, Creighton CJ, Yu Z, Zhu H, Gunaratne PH, Reid JG, Olokpa E, Itamochi H, Ueno NT, Hawkins SM, Anderson ML, Matzuk MM (2010) A link between mir-100 and FRAP1/mTOR in clear cell ovarian cancer. *Mol Endocrinol* 24(2): 447–463.

Potkin SG, Turner JA, Guffanti G, Lakatos A, Fallon JH, Nguyen DD, Mathalon D, Ford J, Lauriello J, Macciardi F. Fbirn (2009) A genome-wide association study of schizophrenia using brain activation as a quantitative phenotype. *Schizophr Bull* 35(1): 96–108.

Rajewsky N (2006) microRNA target predictions in animals. *Nat Genet* 38(Suppl): S8–S13.

Sapi E, Alvero AB, Chen W, O'Malley D, Hao XY, Dwipoyono B, Garg M, Kamsteeg M, Rutherford T, Mor G (2004) Resistance of ovarian carcinoma cells to docetaxel is XIAP dependent and reversible by phenoxodiol. *Oncol Res* 14(1112): 567–578.

Sapranauskas R, Gasiunas G, Fremaux C, Barrangou R, Horvath P, Siksnys V (2011) The *Streptococcus thermophilus* CRISPR/Cas system provides immunity in *Escherichia coli*. *Nucleic Acids Res* 39(21): 9275–9282.

Sasaki H, Sheng Y, Kotsuji F, Tsang BK (2000) Down-regulation of X-linked inhibitor of apoptosis protein induces apoptosis in chemoresistant human ovarian cancer cells. *Cancer Res* 60(20): 5659–5666.

Shibata H, Yamamoto K, Sun Z, Oka A, Inoko H, Arinami T, Inada T, Ujike H, Itokawa M, Tochigi M, Watanabe Y, Someya T, Kunugi H, Suzuki T, Iwata N, Ozaki N, Fukumaki Y (2013) Genome-wide association study of schizophrenia using microsatellite markers in the Japanese population. *Psychiatr Genet* 23(3): 117–123.

Takwi AA, Wang YM, Wu J, Michaelis M, Cinatl J, Chen T (2014) miR-137 regulates the constitutive androstane receptor and modulates doxorubicin sensitivity in parental and doxorubicin-resistant neuroblastoma cells. *Oncogene* 33(28): 3717–3729.

Tamm I, Kornblau SM, Segall H, Krajewski S, Welsh K, Kitada S, Scudiero DA, Tudor G, Qui YH, Monks A, Andreeff M, Reed JC (2000) Expression and prognostic significance of IAP-family genes in human cancers and myeloid leukemias. *Clin Cancer Res* 6(5): 1796–1803.

Ulybina YM, Kuligina ES, Mitiushkina NV, Sherina NY, Baholdin DV, Voskresenskiy DA, Polyakov IS, Togo AV, Semiglazov VF, Imyanitov EN (2011) Distribution of coding apoptotic gene polymorphisms in women with extreme phenotypes of breast cancer predisposition and tolerance. *Tumori* 97(2): 248–251.

van Jaarsveld MT, Helleman J, Boersma AW, van Kuijk PF, van Ijcken WF, Despierre E, Vergote I, Mathijssen RH, Berns EM, Verweij J, Pothof J, Wiemer EA (2013) miR-141 regulates KEAP1 and modulates cisplatin sensitivity in ovarian cancer cells. *Oncogene* 32(36): 4284–4293.

Wang Y, Mao H, Hao Q, Wang Y, Yang Y, Shen L, Huang S, Liu P (2012) Association of expression of XIAP-associated factor 1 (XAF1) with clinicopathologic factors, overall survival, microvessel density and cisplatin-resistance in ovarian cancer. *Regul Pept* 178(1-3): 36–42.

Wu S, Huang S, Ding J, Zhao Y, Liang L, Liu T, Zhan R, He X (2010) Multiple microRNAs modulate p21Cip1/Waf1 expression by directly targeting its 3′ untranslated region. *Oncogene* 29(15): 2302–2308.

Xie Y, Tobin LA, Camps J, Wangsa D, Yang J, Rao M, Witasp E, Awad KS, Yoo N, Ried T, Kwong KF (2013) MicroRNA-24 regulates XIAP to reduce the apoptosis threshold in cancer cells. *Oncogene* 32(19): 2442–2451.

Xu W, Liu M, Peng X, Zhou P, Zhou J, Xu K, Xu H, Jiang S (2013) miR-24-3p and miR-27a-3p promote cell proliferation in glioma cells via cooperative regulation of MXI1. *Int J Oncol* 42(2): 757–766.

Yang H, Kong W, He L, Zhao JJ, O'Donnell JD, Wang J, Wenham RM, Coppola D, Kruk PA, Nicosia SV, Cheng JQ (2008) MicroRNA expression profiling in human ovarian cancer: miR-214 induces cell survival and cisplatin resistance by targeting PTEN. *Cancer Res* 68(2): 425–433.

Zhang P, Li C, Zhang R, Zhang W, Jin C, Wang L, Song L (2015) The roles of two miRNAs in regulating the immune response of sea cucumber. *Genetics* 201(4): 1397–1410.

Zheng T, Wang J, Chen X, Liu L (2010) Role of microRNA in anticancer drug resistance. *Int J Cancer* 126(1): 2–10.

Zhou J, Wang W, Gao Z, Peng X, Chen X, Chen W, Xu W, Xu H, Lin MC, Jiang S (2013a) MicroRNA-155 promotes glioma cell proliferation via the regulation of MXI1. *PloS one* 8(12): e83055.

Zhou P, Xu W, Peng X, Luo Z, Xing Q, Chen X, Hou C, Liang W, Zhou J, Wu X, Songyang Z, Jiang S (2013b) Large-scale screens of miRNA-mRNA interactions unveiled that the 3′UTR of a gene is targeted by multiple miRNAs. *PLoS One* 8(7): e68204.

Zhu W, Xu H, Zhu D, Zhi H, Wang T, Wang J, Jiang B, Shu Y, Liu P (2012) miR-200bc/429 cluster modulates multidrug resistance of human cancer cell lines by targeting BCL2 and XIAP. *Cancer Chemother Pharmacol* 69(3): 723–731.

Supplementary Information accompanies this paper on British Journal of Cancer website (http://www.nature.com/bjc)